Carbonates Evaporites (2013) 28:111–117
DOI 10.1007/s13146-013-0146-5

ORIGINAL ARTICLE

Study of canopy transpiration based on a distributed hydrology model in a small karst watershed of southwest China

Zhi-cai Zhang · Xi Chen · Peng Shi · Geng-xin Ou

Accepted: 2 February 2013 / Published online: 8 March 2013

Abstract Understanding temporal and spatial distribution of canopy transpiration is indispensable in hydrology and hydroecology. Canopy transpiration in a karst basin is controlled by meteorological conditions, plant species, and water in soil and rock fractures. Estimation of canopy transpiration at catchment scale in such heterogeneously hydrogeological conditions is challenging. Hydrological modeling is a useful method to estimate canopy transpiration at catchment scale, and it can be used to evaluate the effect of land-cover change. In this study, a distributed hydrological model was used to estimate canopy transpiration within a small karst watershed for the period July 28, 2007, to October 19, 2007. The results show that transpiration was about 19.2 percent of total rainfall, and daily transpiration rate in this basin ranged from 0.01 to 3.4 mm/day with an average of 0.8 mm/day during the study period. Epikarst water is an important water source for canopy transpiration in addition to soil water in the karst basin. And land-cover change has important effects on canopy transpiration in this area.

Keywords Canopy transpiration · Distributed hydrology model · Karst · Epikarst

Z. Zhang (✉) · X. Chen · P. Shi
State Key Laboratory of Hydrology-Water Resources and Hydraulic Engineering, Hohai University, Nanjing 210098, China
e-mail: zhangzhicai_0@hhu.edu.cn

G. Ou
School of Natural Resources, University of Nebraska-Lincoln, Lincoln, NE 68583-0996, USA

Introduction

Karst terrain covers about 15 % of the world's land area, about 2.2 million km^2, and is home for around 1 billion people (17 % of the world's population) (Yuan and Cai 1988). Understanding of temporal and spatial dynamics of canopy transpiration is crucial for the investigation of ecological and hydrological processes in karst areas. Because the surface soil layer in karst area is usually thin, epikarst zones with fractures are keys for water storage and movement as well as for transpiration of vegetation. According to Xiang et al. (2004), most plants have shallow roots less than one meter deep. Tree roots seldom extend deeper than several meters in karst due to bedrock, with 70 % concentrated within 30 cm of the ground surface. Soil water and epikarst water are primary water sources for plants in the karst forest area. The proportion of plant uptake of epikarst water is about 50 % for the forest and about 35 % for the shrub according to isotope analysis of water sources of forest vegetation on the south China karst plateau (Wang et al. 2008).

The transpiration depends on several properties of the soil–plant–atmosphere continuum. Since the transpiration is often limited by the soil water availability, the prominent environmental factors are the water content and water potential of the soil root zone (Denmead and Shaw 1962). Transpiration has been frequently measured using the sap flow technique applied to field crops (Jara et al. 1998), herbaceous plants (Baker and van Bavel 1987), and trees (Sturm et al. 1996; Lagergren and Lindroth 2002). Direct measure of canopy transpiration usually does not consider the processes of soil moisture and it is at point scale, but information for larger areas is often required. Estimating transpiration at the catchment scale is a significant challenge. Mu et al. (2009) developed a method to use remote

sensing data from satellites to compute actual transpiration. To be useful, however, this method needs to be updated frequently. A complementary technique is to use a hydrological model, which can simulate the complete components in the hydrological cycle, to estimate canopy transpiration. In karst areas especially, water uptake for canopy transpiration depends on plant species and water in soil and rock fractures. Interactions of transpiring plants with water in soil and rock fractures could be quantified by means of hydrological modeling (Kite 2000).

In this study, a distributed hydrological model was used to estimate canopy transpiration and understand transpiration responses to land use change for a small watershed of Chenqi within the Puding Karst Ecohydrological Observation Station, Guizhou Province of China (Fig. 1).

Materials and methods

The distributed hydrological model

The distributed hydrological model was developed by Zhang et al. (2011), based on the distributed hydrology–soil–vegetation model (DHSVM, Wigmosta et al. 1994). The model was designed for porous and fissured media in karst terrains. Infiltration and saturated flow movement within epikarst fractures were modeled with the cubic law equation which is associated with fracture width, direction, and spacing.

Based on the original DHSVM structure, a multi-layer model is used for accounting soil moisture and epikarstic flow dynamics:

$$d_1(\theta_1^{t+\Delta t} - \theta_1^t) = P_0 - P_1(\theta_1) - E_{\text{to}} - E_{\text{tu}} - E_s + V_{\text{sat}} - V_r \quad (1)$$

$$d_2(\theta_2^{t+\Delta t} - \theta_2^t) = P_1(\theta_1) - P_2(\theta_2) - E_{\text{to}} + V_{\text{sat}} \quad (2)$$

$$d_3(\theta_3^{t+\Delta t} - \theta_3^t) = P_2(\theta_2) - P_3(\theta_3) + (Q_{\text{sin}}^t - Q_s^t)\Delta t \quad (3)$$

where d_1 and d_2 are soil and epikarst thickness of the upper and lower rooting zones, respectively, d_3 is the left epikarst thickness perched by saturated water, θ_n ($n = 1, 2, 3$) is the average soil moisture content (SMC) of the nth zone, P_0 is the volume of infiltrated rainfall, V_{sat} is the volume of water supplied by a rising water table, V_r is the volume of return flow, E_{to} and E_{tu} are evapotranspiration from overstory vegetation (o) and understory vegetation (u), respectively. Evapotranspiration (E_{to}) for vegetation root uptake from the upper and lower layers is usually dependent on density of root extension. E_s is soil evaporation, $P_n(\theta)$ ($n = 1,2,3$) is downward volumes of water discharged from nth zones over the time step, Q_{sin}^t and Q_s^t are the subsurface flow rates to pass in and out the epikarst zone, respectively.

An equivalent hydraulic conductivity $K_v(\theta)$ as follows could be used to compute infiltration and percolation $P_n(\theta)$ based on Darcy's law assuming a unit hydraulic gradient:

$$P_n(\theta) = K_v(\theta) \quad (4)$$

For the uppermost soil,

$$K_v(\theta) = K_v(\theta_s)\left[\frac{\theta - \theta_r}{\varphi - \theta_r}\right]^{(2/m)+3} \quad (5)$$

where m is the pore size distribution index, ϕ is the soil porosity, and θ_r is the residual SMC. For simplicity, the saturated moisture content θ_s is taken equal to ϕ.

The equivalent hydraulic conductivity of a rock mass with one parallel set of fractures with rough surface is expressed by:

$$K_{i,j} = C\frac{\rho g b_{i,j}^3}{12\mu s} \quad (6)$$

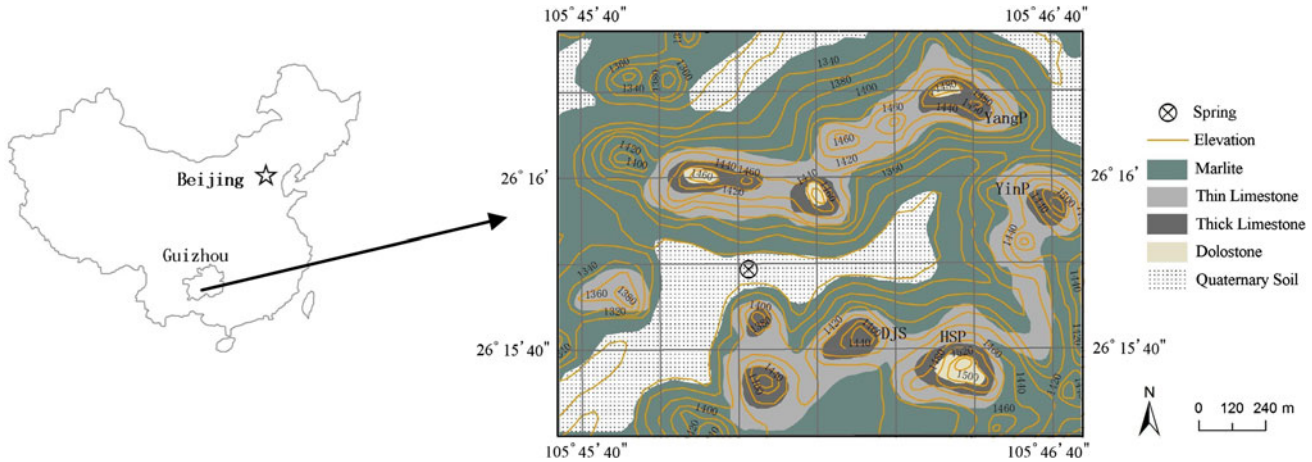

Fig. 1 Topography and geology in Chenqi basin

where s is the fracture spacing (m), C is a coefficient which is related with the roughness of the fracture surfaces and fracture aperture.

For the uppermost soil zone with partially rock exposure, an equivalent infiltration rate can be estimated by the following equation:

$$P_{n,\mathrm{eq}}(\theta_n) = K_v(\theta)(1 - f_r) + K_{i,j} f_r \tag{7}$$

where f_r is the ratio of rock exposure.

In the saturated epikarst zone, subsurface water flowing cell by cell is calculated by the following equation with different values of horizontal transmissivities.

$$q(t)_{i,j,k} = w_{i,j,k} f_{i,j,k} T(t)_{i,j} \tag{8}$$

$$T(t)_{i,j} = \frac{Ks_{i,j}}{\alpha_{i,j}} (e^{-\alpha_{i,j} z_{i,j}} - e^{-\alpha_{i,j} D_{i,j}}) \tag{9}$$

where $w_{i,j,k}$ is the grid (i, j) width at k flow direction, $T(t)_{i,j}$ is the hydraulic transmissivity for grid (i, j), $f_{i,j,k}$ is the flow fraction for cell i, j in direction k and is usually estimated as topographic slope or groundwater slope $\beta_{i,j,k}$, $Ks_{i,j}$ is the lateral component of saturated hydraulic conductivity for cell i, j at epikarst surface and is estimated by Eq. (8) with horizontal fractural aperture and spacing, $z_{i,j}$ is the distance from the epikarst surface to the water table (positive downward), $\alpha_{i,j}$ is a parameter related to the decay of saturated conductivity with depth, and $D_{i,j}$ is the total epikarst depth.

For a soil matrix, lateral flow direction in the subsurface depends on hydraulic gradient which is usually assumed as the topographic slope and isotropic hydraulic transmissivity $T_{i,j}$ at cell i, j. In karst basins, however, subsurface water in karstic aquifers moves through an interconnected system of fractures, and strong anisotropy of karst fracture dominates subsurface flow directions as well (Scanlon et al. 2003; Xue et al. 2009). Equation (8) for subsurface water flow at cell i, j in flow direction k should therefore be revised as.

$$q(t)_{i,j,k} = w_{i,j,k} f_{i,j,k} T(t)_{i,j,k} \tag{10}$$

where $T(t)_{i,j,k}$ is hydraulic transmissivity for cell (i, j) at k flow direction and can be expressed as $p_{i,j,k} \sum_{k=1}^{8} T_{i,j,k}$ in which $p_{i,j,k}$ is equal to $\frac{T_{i,j,k}}{\sum_{k=1}^{8} T_{i,j,k}}$, representing karst fractural anisotropy for cell i, j in direction k. Hence, the following formula was developed to calculate flow fraction $f_{i,j,k}$ for cell i,j in direction k, considering topographic slope or groundwater slope $\beta_{i,j,k}$ and aquifer anisotropy $p_{i,j,k}$:

$$f_{i,j,k} = p_{i,j,k} \beta_{i,j,k} \tag{11}$$

Since the exact location, geometry, and hydraulic properties of each fracture are usually unknown, a stochastic model was applied to describe statistical attributes of rock fractures. In the absence of field description of fractural anisotropy, the weight $p_{i,j,k}$ can be randomly generated on the basis of uniform distribution of p value between 0 and 1 in eight directions (Xue et al. 2009).

In this model, flow in the conduit systems is routed using a series of cascading, linear channel reaches. Each reach was described with hydraulic parameters. As the reach passes through grid cells, lateral inflow of the channel reach consists of the matrix and fracture flow. Flow is routed between channel reaches with a linear routing algorithm, treating each reach as a reservoir of constant width and with outflow linearly related to storage.

$$Q_{\mathrm{out}} = Q_{\mathrm{in}} - (V_C^{t+1} - V_C^t)/\Delta t \tag{12}$$

$$V_C^{t+1} = \frac{Q_{\mathrm{in}}}{k} + (V_C^t - \frac{Q_{\mathrm{in}}}{k}) \exp(-k\Delta t) \tag{13}$$

$$k = \frac{R_r^{2/3} \sqrt{S_o}}{n \Delta L} \tag{14}$$

where k is a coefficient of underground channel storage, R_r is the hydraulic radius, S_o is hydraulic gradient, ΔL is the length of channel segment, n is the manning's roughness coefficient, and Δt is time step. V_c is channel reach storage, Q_{out} is the average outflow from the reach, Q_{in} is the average rate of lateral and upstream inflow to the reach during the time step.

Study site

The 1.5-km^2 Chenqi study basin is located in the Puding county of Guizhou Province of China. The study site has a subtropical wet monsoon climate with a mean annual temperature of 20.1 °C and annual precipitation of 1,140 mm. The bedrock is dolomite, thick and thin limestone, and marlite and quaternary soil.

The plant species include grasses, karst montane deciduous broad-leaved shrubs and evergreens, and deciduous broad-leaved mixed forest (Fig. 2a). According to the field investigation by Peng et al. (2008), in the forest area of Yinpo (YinP) and Dongjiashan (DJS), tree height varies from 2 to 5 m and canopy fraction is about 80–90 % with 20–40 % rock exposure. In the shrub area of Yangpo (YangP) and Huoshaopo (HSP), tree height varies from 1 to 1.5 m and canopy fraction is about 20–50 % with 30–50 % rock exposure. In the grass area, the canopy fraction is about 80 % with 35 % rock exposure.

Distribution of soil properties (types, composition and density) is determined through field investigation and laboratory experiments on 49 soil samples. Generally, soil of the upper 20 cm is classified into two types: loam in the low and depression areas and sand loam in the middle and

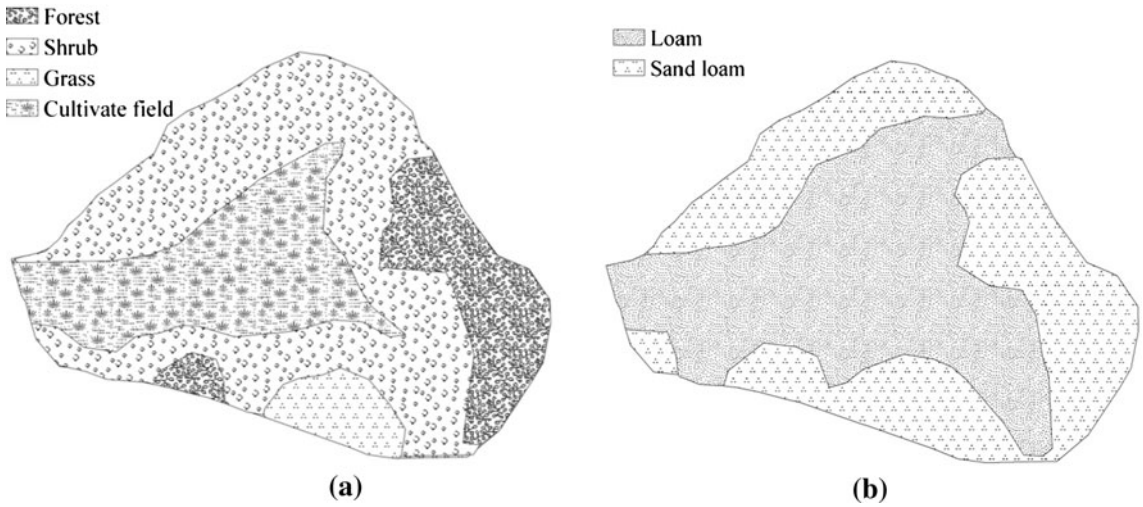

Fig. 2 Vegetation (**a**) and soil (**b**) maps

upper hillslope areas (Fig. 2b), with bulk density of 0.66–0.90 g/cm^3 and porosity of 0.2–0.4, respectively. The lower layer is primarily brown clay with high calcium content (Fig. 2b). The clay has a density of 1–1.28 g/cm^3 and porosity of 0.42–0.48. On most hillslopes, soil is usually thin and less than 50-cm thick. Agricultural soils are generally deeper than 2 m.

Meteorological data

In this study, a period between July 28 and October 19, 2007, was selected for the investigation of transpiration and its association with meteorological conditions and land cover. During this period, total rainfall was 338 mm and the maximum hourly rainfall rate was 86 mm/h. The mean, maximum, and minimum air temperatures were 18.6, 29.6, and 9.4 °C, respectively. The mean, maximum, and minimum irradiances were 281, 1,058, and 0.6 w/m^2, respectively. The mean wind speed and relative humidity were 0.93 m/s and 85.8 %, respectively.

Results and discussion

The model was applied to the Chenqi basin for the period July 28, 2007, to October 19, 2007, by Zhang et al. (2011). The model parameters were determined on the basis of field measurements and calibration against the observed soil moisture contents, vegetation interception, surface runoff, and underground flow discharge from the basin outlet. The improved model generally reproduced temporal variations in flow discharge at the underground outlet of Chenqi catchment with the coefficient of determination of larger than 0.75 (Zhang et al. 2011).

Estimation of canopy transpiration

The model calculated 0.56 mm of average daily actual transpiration (AT) during the period July 28, 2007, to October 19, 2007, for the study basin. The total actual transpiration calculated by this model is 65.1 mm in the watershed, and it is about 19.2 % of the rainfall amount during this period.

Mean daily actual transpiration in August was modeled to be 1.2 mm, about three times as the daily rate in September and October (0.4 mm) (Fig. 3). Actual transpiration varied with land cover. Forest transpiration (1.3 mm) was modeled to be much larger than that of shrub (0.4 mm) and grass areas (0.1 mm; Fig. 3).

Relationship between actual transpiration and potential transpiration

In the model, potential transpiration (PT) was estimated with the Penman–Monteith (P–M) equation (Monteith

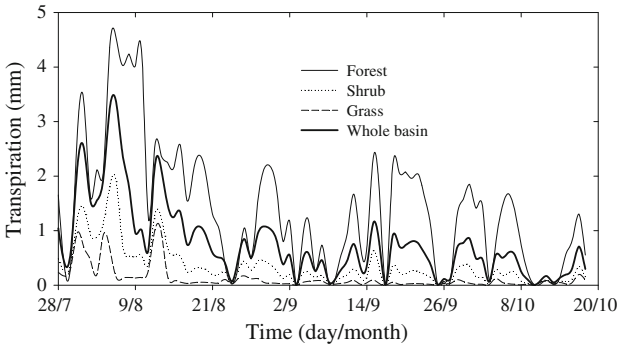

Fig. 3 Average transpiration in the whole basin, forest, shrub, and grass area

1965). Comparison of actual to potential transpiration was made in a successive 6-day no-rainfall period from August 5–10. In the first 3 days (August 5–7), basin mean actual transpiration was close to potential transpiration when sufficient water was stored and available in the soil and fracture zones (Fig. 4). Actual and potential transpiration were significantly different from August 8–10 when the mean soil moisture contents decreased. The highest rates of actual transpiration on August 8, 9, and 10 were 0.2, 0.1, and 0.1 mm/h, respectively: smaller than the highest rate of potential transpiration of 0.4 mm/h during these 3 days.

Estimated transpiration from the rooted zone of soil and epikarst zones

Water uptake by plants is related to the distribution of roots in soils and fractures. According to Xiang et al. (2004), Wang et al. (2008), and the authors' field investigations, root distribution in the upper soil layer of 0–20 cm, lower soil layer of 20–50 cm, and underlying epikarst zone is 20, 40, and 40 %, respectively, for forest, 70, 30, and 0 %, respectively, for shrub, and 90, 10, and 0 %, respectively, for grass.

The moisture content of 0.34 in the lower soil layer (modeled and averaged over the basin for the study period) was much larger than in the upper soil layer and epikarst with the soil moisture content of 0.14 and 0.02, respectively. Higher fluctuation of soil moisture content was obtained in the upper soil layer in response to rainfall and temperature (Fig. 5a).

The value of wilting moisture content (θ_w) subtracted from soil moisture content (θ) multiplied by soil and epikarst thickness (D) represents the available water for plant uptake in the root zone. Wilting moisture content was determined by field experiments and laboratory analysis, and soil moisture content in each time step can be calculated by modeling. Results indicate that the lower soil layer has a larger available water of 286 mm during the study period, and available water is 46 mm in the upper layer of soil and 116 mm in the epikarst zone (Fig. 5b).

Land-cover changes and effects on canopy transpiration

Due to some human activities, land degradation involving severe soil erosion and extensive exposure of basement rocks is the essential environmental problem in southwest China. In this study, variations of canopy transpiration were simulated for some land-cover scenarios and estimated the effects of land use change on canopy transpiration at the catchment scale.

Rock exposure rate scenario

According to the field investigation by Peng et al. (2008), the mean rock exposure rate in this basin is about 36 %. Two scenarios, which increase and decrease the catchment exposure rate by 20 %, were prescribed. The catchment exposure rate was modeled as 43 and 29 %, respectively. Under the higher scenario, the actual transpiration, soil evaporation, and evapotranspiration simulated with the model decreased by 7.5, 13.1, and 7.3 %, respectively. Under the lower rock exposure scenario, mean actual transpiration, soil evaporation, and evapotranspiration simulated with the model in this catchment increased by 7.7, 11.2, and 7.1 %, respectively (Table 1).

When the exposure rate increases, the water used for canopy transpiration and soil evaporation decreases, and more rainfall infiltrates into fractures. In this condition, more water discharges as conduit runoff, hindering the vegetation recovery in karst area.

Soil depth scenario

Soil erosion is another common phenomenon in the karst area in southwest China. Soils in this karst region, developed on carbonate rocks, are generally thin (30- to 50-cm

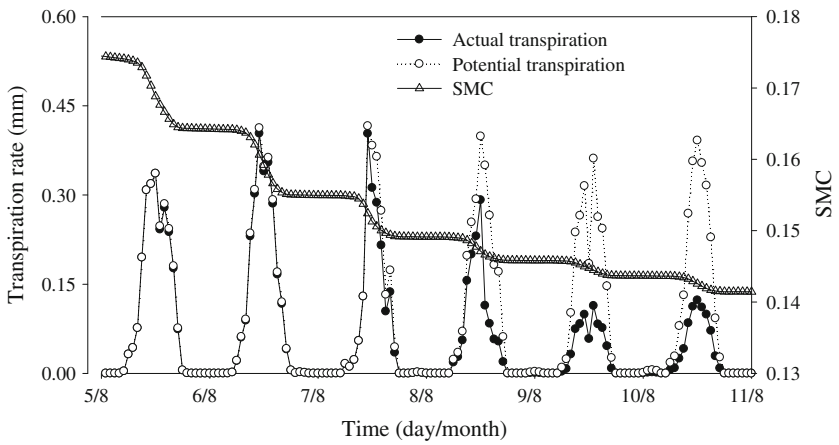

Fig. 4 Basin average AT and PT during August 5–10

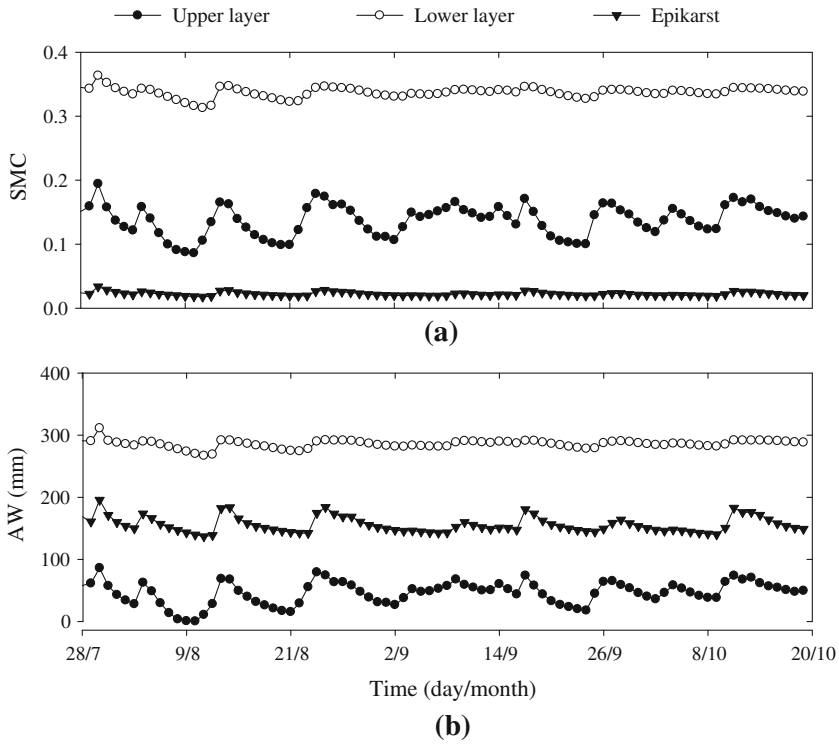

Fig. 5 Variation of moisture contents (**a**), and AWR (**b**)

Table 1 Modeled evapotranspiration under different exposure rate scenarios

Exposure rate	AT (mm)	E_s (mm)	E_i (mm)	ET (mm)
Now (36 %)	65.1	22.2	19.0	106.3
Increase 20 %	60.2 (−7.5 %)	19.3 (−13.1 %)	19.0	98.5 (−7.3 %)
Decrease 20 %	70.1 (+7.7 %)	24.7 (+11.2 %)	19.0	113.8 (+7.1 %)

thick). Soil erosion has converted 5,000 km^2 into karst desert in Guizhou Province, which makes the restoration of vegetation very difficult due to little or no soil remaining. It takes 2,000–8,000 years for weathering of carbonate rock to produce 1 cm of soil in some karst areas because very little soluble material is left after dissolution (Li et al. 2002).

To estimate the effects of soil erosion on transpiration, scenarios of different soil depths were used. In this study, the variation in soil physical and chemical properties was not considered. In this basin, mean soil depths are 32 and 200 cm on hillslopes and depression areas, respectively. When mean soil depth in this basin decreases 10 cm, the simulated actual transpiration, soil evaporation, and evapotranspiration decrease by 10.2, 21.3, and 10.7 %, respectively. On the contrary, with an increase of 10 cm of soil depth, simulated actual transpiration, soil evaporation, and evapotranspiration increase by 6.8, 12.5, and 6.8 %, respectively (Table 2). The results show that soils play an important role in the water cycle, especially in the high-evapotranspiration karst area, and water storage capacity of the catchment will be reduced when soil depth decreases.

Forest degradation scenario

In karst areas of southwest China, cultivated lands usually are located on slopes. For example, in Guizhou Province, at present, 81 % of cultivated land in the province is on slopes of 6° or more. Cultivated land on slopes over 25° accounts for about 20 % of the total cultivated land area. Cultivated land on slopes over 35° accounts for about 6 %. People in this area usually burn mountain forests to get more cultivated land. Some forests degenerate to grassland after these actions. Deforestation occurred in the Chenqi basin in 2007. Currently, forest areas account for 27 % of the area in the basin, and the scenario of all forests in this basin was set to degenerating to grassland. The simulated actual transpiration, E_i, and evapotranspiration decrease by 27.5, 35.8, and 15.9 %, respectively (Table 3). Once the forest is removed, more soil will lose the vegetation shelter, therefore increasing soil evaporation (by about 34.4 % in this case). Thus, deforestation increases the risk of soil erosion in this region.

Conclusions

In this study, a hydrological model was used to simulate the canopy transpiration in a small watershed of Chenqi

Table 2 Modeled evapotranspiration under different soil depth scenarios

Soil depth	AT (mm)	E_s (mm)	E_i (mm)	ET (mm)
Now: hillslopes: 32 cm depression areas: 200 cm	65.1	22.2	19.0	106.3
Decrease 10 cm	58.4 (−10.2 %)	17.5 (−21.3 %)	19.0	94.9 (−10.7 %)
Increase 10 cm	69.5 (+6.8 %)	25.0 (+12.5 %)	19.0	113.5 (+6.8 %)

Table 3 Modeled evapotranspiration under forest degradation scenario

Land use	AT (mm)	E_s (mm)	E_i (mm)	ET (mm)
Now (27 %)	65.1	22.2	19.0	106.3
Forest → grassland	47.2 (−27.5 %)	15.1 (+34.4 %)	19.6 (−35.8 %)	103.0 (−15.9 %)

within the Puding Karst Ecohydrological Observation Station, Guizhou Province of China. The application of this distributed hydrological model is an effective tool to analyze transpiration processes for karst catchments. In addition to soil water, the study suggests fracture water is an important source of water for transpiration in karst area. Transpiration is influenced mostly by meteorological conditions when available water in soil and fractures is sufficient. Most transpiration is from the upper soil layer when soils are wet. As soil moisture decreases, plants tend to take more water from the lower soil layers and the epikarst zone. Variation of canopy transpiration was investigated with the hydrological model for different land-cover scenarios. The results show that land-cover changes have significant effects on canopy transpiration in karst area.

Acknowledgments This research was supported by National Basic Research Program of China (973 Program) (no. 2006CB403200), National Natural Scientific Foundation of China (no. 40930635, and 41101018), the Key Project of China Ministry of Education (no. 308012), Programme of Introducing Talents of Discipline to Universities (no. B08048) and Program for Changjiang Scholars and Innovative Research Team in University, China.

References

Baker JM, van Bavel CHM (1987) Measurements of mass flow of water in the stems of herbaceous plants. Plant Cell Environ 10(9):777–782

Denmead OT, Shaw RT (1962) Availability of soil water to plants as affected by soil moisture content and meteorological conditions. Agron J 54:358–390

Jara J, Stockle CO, Kjelgaard J (1998) Measurement of evapotranspiration and its components in a corn (Zea Mays L.) field. Agric For Meteorol 92(2):131–145

Kite G (2000) Using a basin-scale hydrological model to estimate crop transpiration and soil evaporation. J Hydrol 229(1):50–69

Lagergren F, Lindroth A (2002) Transpiration response to soil moisture in pine and spruce trees in Sweden. Agric For Meteorol 112(2):67–85

Li R, Wang S, Zhang D (2002) The role of man-made factors in ecoenvironmental detection in Guizhou karst areas. Bull Miner Petrol Geochem 21(1):43–47

Monteith JL (1965) Evaporation and environment. In: Fogg GE (ed.) The state and movement of water in living organisms. University Press, Cambridge, pp 205–234

Mu QZ, Jones LA, Kimball JS, McDonald KC, Running SW (2009) Satellite assessment of land surface evapotranspiration for the pan-Arctic domain. Water Resour Res 45(9):W09420

Peng T, Wang SJ, Zhang XB, Rong L, Chen B, Yang T, Wan JY (2008) Results of preliminary monitoring of surface runoff coefficients for karst slopes. Earth and Environment 36(2):25–129 (in Chinese)

Scanlon BR, Mace RE, Barrett ME, Smith B (2003) Can we simulate regional groundwater flow in a karst system using equivalent porous media models? Case study, Barton Springs Edwards aquifer, USA. J Hydrol [Amsterdam] 276(1–4):137–158

Sturm N, Reber S, Kessler A, Tenhunen JD (1996) Soil moisture variation and plant water stress at the Hartheim Scots pine plantation. Theoret Appl Climatol 53(1–3):123–133

Wang S, Rong L, Du X, Ge Y (2008) Water source partitioning and water use strategy among karst trees growing on shallow karst—perspectives from stable isotope composition. Bull Miner Petrol Geochem 27(z1):513–514

Wigmosta MS, Vail LW, Lettenmaier DP (1994) A distributed hydrology-vegetation model for complex terrain. Water Resour Res 30(6):1665–1679

Xiang C, Song L, Zhang P, Pan G, Wang J (2004) Preliminary study on soil fauna diversity in different vegetation cover in Shilin National Park, Yunnan, China. Resour Sci 26:98–103

Xue X, Chen X, Zhang Z, Wei L (2009) Effect of karst fracture on saturated subsurface flow confluence: Water Resour. Power 27(6):20–23 (in Chinese)

Yuan DX, Cai GH (1988) The science of karst environment: Chongqing. Chongqing Press (in Chinese), China

Zhang ZC, Xi C, Ghadouani A, Peng C (2011) Modeling hydrological processes influenced by soil, rock and vegetation in a small karst basin of southwest China. Hydrol Process 25(15):2456–2470